

# PHOTOVOLTAIC GENERATOR MODELLING FOR POWER SYSTEM SIMULATION STUDIES

Anna Rita Di Fazio, Mario Russo  
DAEIMI, Università degli Studi di Cassino  
Cassino, Italy  
a.difazio@unicas.it

**Abstract - PhotoVoltaic (PV) systems are widely spreading in distribution networks and their detailed models are required in power system simulation studies. Some components of PV systems present non-linear characteristics, that may introduce numerical instability problems during power system simulation. In particular, the model of the PV generator introduces a non-linear dependency of the injected current on the terminal voltage. The paper investigates the numerical instability problems caused by the PV generator model. To overcome such problems while keeping high computational efficiency of the simulation, a new representation of the PV generator model is proposed. It can be efficiently included into power system simulation based on EMTP and EMTDC and its validity is tested using PSCAD/EMTDC tool.**

**Keywords - Grid connected photovoltaic system, Photovoltaic generator, Power system simulation, EMTP/EMTDC**

## 1 INTRODUCTION

PHOTOVOLTAIC (PV) systems are widely spreading in distribution networks and attracting a growing amount of political and commercial interest, because they exploit a renewable energy source. To derive components ratings, optimise protection and controller settings, perform economic analysis as well as evaluate the impact on the distribution system operation, detailed modelling of grid connected PV systems for power system simulation studies are needed.

Research has deeply analysed the models for the components of a grid connected PV system, including equivalent circuits of the PV generator [1, 2, 3], configuration and dynamic response of the inverter [4, 5, 6], behavior of the grid interface and performance of the control system [7, 8, 9]. Other important aspects have been addressed, related to the inclusion of the PV system into the distribution network [10, 11, 12, 13]. In this field, minor attention has been paid to the numerical problems that arise during the power system simulation. They are caused by the non-linearities present in the models of some components of a PV system. While numerical problems related to the non-linearities of switching inverters are well treated [14], the ones related to the PV generators have not been analysed and are tackled in this paper.

From a strict mathematical point of view, in each step of the simulation, the set composed of the non-linear equations representing the PV generators and the linear equa-

tions representing the rest of the power system must be solved, using an iterative numerical algorithm. Some power system simulation tools adopt this approach, such as PSpice [15]. This approach is accurate but presents the drawback of a heavy computational burden when simulating large distribution networks including PV systems.

To guarantee computational efficiency a different approach is used by separating the non-linear equations of the PV generators from the linear equations of the rest of the power system. This approach is referred to as Basic Linear System Technique (BLST) in the following and is adopted by power system simulation tools based on EMTP or EMTDC [16]. However, the non-linear equations introduce a dependency of the current injected by the PV generator on the terminal voltage, which in turns is related to the operating conditions of the whole power system. Such a dependency can cause numerical instability of the simulation.

To overcome numerical instability problems, a possible solution is to use the Compensation Method (CM) [17, 18]. This technique, while keeping separated the non-linear equations from the linear ones, includes the Thevenin equivalent circuit of the power system into the PV generator model. The CM avoids any numerical transient but requires the evaluation of the Thevenin equivalent impedance, which is not available in most power system simulation tools.

A new approach is proposed in this paper to overcome most numerical problems while keeping high computational efficiency of the simulation. The basic idea is to extend the original approach of BLST by adding some information extracted from the non-linear equation of the PV generator into the linear equations of the rest of the power system. To this aim, the PV generator model, based on the single-diode equivalent circuit, is modified by proposing a new representation that can be efficiently included into power system simulation tools based on EMTP or EMTDC.

In the paper, at first the classical PV generator model based on the single-diode equivalent circuit is briefly recalled. Secondly, the problems that arise including this model into power system simulation are analysed. Then, the proposed approach, named Extended Linear System Technique (ELST), and the new representation of the PV generator model are presented. Eventually, using PSCAD/EMTDC tool [16, 19], numerical results are reported showing cases in which numerical instability problems are overcome.

## 2 RECALLING THE SINGLE-DIODE EQUIVALENT CIRCUIT

The basic unit of a PV generator is the PV cell. An individual PV cell typically produces from 1 to 2 W. To increase the power, cells are electrically connected to form larger units, called PV modules. In practice, a PV module consists of PV cells connected in series. Modules, in turns, can be connected in series and parallel to form larger units called PV panels. Panels connected in series constitute a PV array. Arrays connected in parallel constitute a PV generator.

The single-diode equivalent circuit is the most commonly adopted model for PV cells, accounting for the photon-generated current and the physics of the  $p-n$  junction of a PV cell [1].

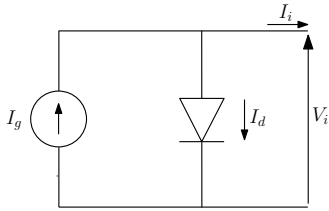


Figure 1: Single-diode equivalent circuit of the ideal PV cell.

Fig. 1 shows the single-diode equivalent circuit of the ideal PV cell, composed of a current source, modelling the photon-generated electron-hole pairs under the influence of the built-in field, and a diode in parallel to the source, modelling the diffusion of minority carriers in the depletion region. The basic equation describing the ideal PV cell is

$$\begin{aligned} I_i(V_i) &= I_g - I_d(V_i) \\ &= I_g - (I_o (e^{\frac{\beta V_i}{a}} - 1)) \end{aligned} \quad (1)$$

where  $I_i$  and  $V_i$  are the terminal current and voltage of the ideal PV cell,  $I_g$  is the current generated by the incident light and  $I_d$  is the current diverted through the diode. The current  $I_d$  is replaced by the Shockley diode equation modified by the ideality factor  $a$ , to take into account the effects of recombination in the depletion region; in (1),  $I_o$  is the diode reverse saturation current, and  $\beta$  is the inverse thermal voltage defined as

$$\beta(T) = \frac{q}{kT} \quad (2)$$

where  $k$  is the Boltzmann constant ( $1.3806503e^{-23}$  J/K),  $q$  is the electron charge ( $1.60217646e^{-19}$  C) and  $T$  is the  $p-n$  junction temperature.

Fig. 2 shows the single-diode circuit of the real PV cell. The model of the ideal PV cell is enriched by the series resistance  $R_s$ , related to structural resistances of the PV cell, and the parallel resistance  $R_p$ , due to the leakage current of the  $p-n$  junction. By using (1) and applying Kirchhoff's laws, the basic equation describing the real PV cell is obtained

$$\begin{aligned} I(V) &= I_i(V) - I_p(V) \\ &= (I_g - I_o (e^{\frac{\beta(V+R_s I)}{a}} - 1)) - \frac{V + R_s I}{R_p} \end{aligned} \quad (3)$$

where  $I$  and  $V$  are the terminal current and voltage of the real PV cell and  $I_p$  is the current diverted through  $R_p$ .

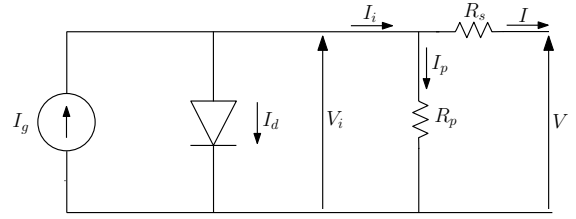


Figure 2: Single-diode equivalent circuit of the real PV cell.

If the five circuit parameters  $a$ ,  $I_g$ ,  $I_o$ ,  $R_s$  and  $R_p$  are related to the PV module, which consists of  $M_s$  series-connected PV cells, equation (3) still holds for the PV module, provided that the inverse thermal voltage in (2) is modified according to

$$\beta(T) = \frac{q}{M_s k T}. \quad (4)$$

In general, all the five circuit parameters are functions of the type of PV device, the solar irradiation  $G$  and the  $p-n$  junction temperature  $T$ . They can be determined on the basis of experimental data or data provided from manufacturers, by using different methods including approximate analytical expressions [2, 20] and accurate empirical model [21]. In this paper, only the dependencies of  $I_g$  and  $I_o$  from the environmental conditions are considered, whereas the dependencies of  $a$ ,  $R_s$  and  $R_p$  are neglected.

The circuit shown in Fig. 2 can also be used to represent a PV generator, composed of  $N_p$  parallel and  $N_s$  series connections of PV modules, which are assumed to be of the same type and in the same environmental conditions. In this case, the five circuit parameters involved in (3) and the inverse thermal voltage in (4) are related to the PV generator and indicated with  $a_{gen}$ ,  $I_{g,gen}$ ,  $I_{o,gen}$ ,  $R_{s,gen}$ ,  $R_{p,gen}$  and  $\beta_{gen}$  respectively. They can be evaluated from the PV module parameters as

$$\begin{aligned} a_{gen} &= a & I_{g,gen} &= N_p I_g & I_{o,gen} &= N_p I_o \\ R_{s,gen} &= \frac{N_s}{N_p} R_s & R_{p,gen} &= \frac{N_s}{N_p} R_p & \beta_{gen} &= \frac{\beta}{N_s}. \end{aligned} \quad (5)$$

On the other hand, the single-diode equivalent circuit can always be used to represent a group of PV modules of the same type and in the same environmental conditions, and various circuits can be electrically connected to form the whole PV generator.

## 3 INCLUDING THE PV GENERATOR MODEL IN THE SIMULATION

The PV generator model, based on the single-diode equivalent circuit, is essentially a non-ideal current generator: it injects a current  $I$  whose value depends on the PV terminal voltage  $V$ , which, in turns, depends on the operating conditions of the whole power system which the PV generator is connected to.

For the sake of simplicity and clarity, but without any loss of generality, the following assumptions are adopted:

- the PV generator is composed of modules of the same type and in the same environmental conditions;
- the power system is assumed to be linear except for the presence of the PV generator;
- the parameters  $R_s$  and  $R_p$ , being constant, are included into the model of the linear power system; then, the non-linear component is reduced to the ideal PV generator in Fig. 1.

To explain the problems arising in simulation and to illustrate the proposed solution, a simple circuit, representing an ideal PV generator supplying a resistive load  $R_e$ , is used as example case (Fig. 3).

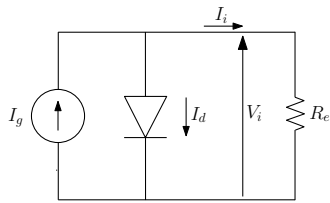


Figure 3: Ideal PV generator supplying a resistive load.

From a strict mathematical point of view, in each step of the simulation, the set composed of the non-linear equation of the ideal PV generator and of the linear equations representing the rest of the power system must be solved using an iterative numerical algorithm, typically based on the Newton-Raphson technique. Some power system simulation tools adopt this approach, such as PSpice.

Referring to the example case in Fig. 3, in the  $k$ th step of simulation the following non-linear problem should be solved

$$V_i(k) = R_e I_i(V_i(k)) \quad (6)$$

where  $I_i(V_i(k))$  is given by (1).

This method is accurate but presents the drawback of a heavy computational burden when simulating large distribution networks including several PV systems. Numerical instability may arise inside the iterative numerical algorithm that solves the set of linear and non linear equations, but the Newton-Raphson techniques are nowadays enhanced to be quite robust.

To guarantee computational efficiency, a different approach can be adopted by separating the non-linear equation of the ideal PV generator from the linear equations of the rest of the power system, namely the BLST. The block diagram related to the  $k$ th step of the simulation is represented in Fig. 4. In details, the value  $I_i(k)$  is evaluated by (1) given the value  $V_i(k-1)$  available from the previous step of the simulation. Then, the linear power system is solved, assuming a current injection equal to  $I_i(k)$  in place of the PV generator. The resulting vector  $\mathbf{V}(k)$  represents the values of all nodal voltages, which also includes the value  $V_i(k)$  of the voltage at the PV generator terminal. The BLST is adopted by various power system simulation tools, such as the ones based on EMTP and EMTDC.

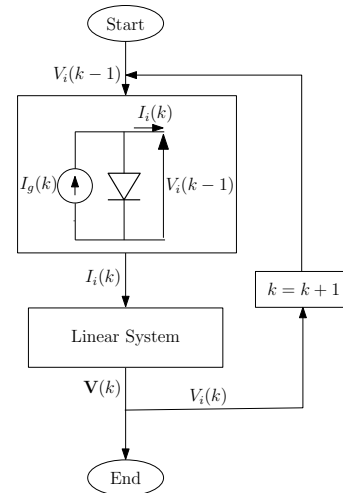


Figure 4: Block diagram of the simulation steps in case of BLST.

The BLST presents a computational burden which is comparable with the one of linear power systems. However, the non-linear equation introduces a strict dependence of the PV generator performance on the operating conditions of the whole power system, which can cause numerical instability in the simulation.

Referring to the example case in Fig. 3, the  $k$ th step of the simulation results into

$$V_i(k) = R_e I_i(V_i(k-1)) \quad (7)$$

which is the zero order approximation of the Taylor series of (6). The numerical instability is due to the one-step delayed value  $V_i(k-1)$  used in (7). An approximated sufficient condition for convergence to be satisfied at each step of the simulation is

$$\frac{1}{R_e} > \left| \frac{\partial I_i(V_i)}{\partial V_i} \Big|_{V_i(k-1)} \right|. \quad (8)$$

This condition is derived in the Appendix.

To overcome numerical problems in BLST, a possible solution is to include the Thevenin equivalent circuit of the power system, as seen from the PV generator terminals, into the PV generator model, namely the CM. The block diagram related to the  $k$ th step of the simulation is represented in Fig. 5. In details, at first the linear power system is solved assuming no current injection from the PV generator. The resulting vector  $\mathbf{V}^o(k)$  represents the values of all nodal voltages in absence of the PV generator. It also includes the voltage  $V_i^o(k)$  calculated at the PV generator terminals, which coincides with the open-circuit voltage of the Thevenin equivalent circuit. The network solution also provides the value of the Thevenin equivalent impedance  $Z_i^{Th}(k)$  as seen from the PV generator terminals. In the second block, the value  $I_i(k)$  is evaluated by using an iterative numerical algorithm that solves the non linear circuit composed of the PV generator and the Thevenin equivalent. In the third block, the linear power system is solved assuming the PV generator current injection  $I_i(k)$  as the only enforcement. The

result is the vector  $\mathbf{V}^{I_i}(k)$  of nodal voltages in presence of the only PV generator. Eventually, the vector  $\mathbf{V}(k)$  of nodal voltages is obtained by superimposing the effects:  $\mathbf{V}(k) = \mathbf{V}^o(k) + \mathbf{V}^{I_i}(k)$ .

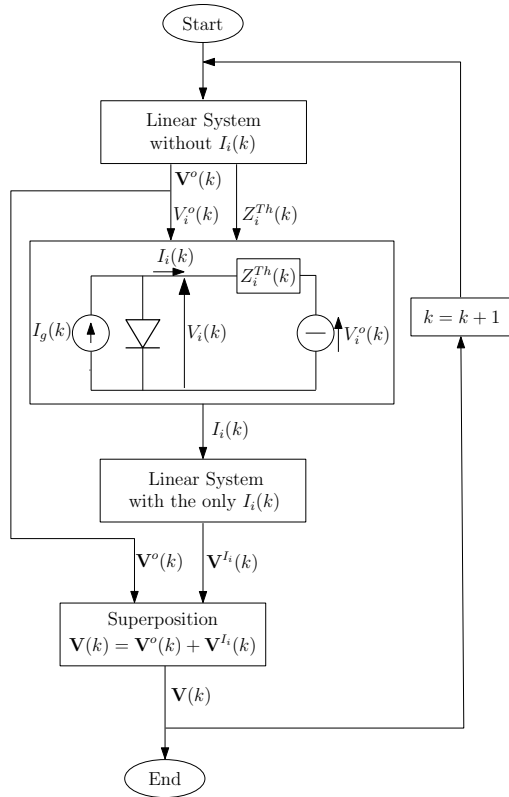


Figure 5: Block diagram of the simulation steps in case of CM.

Referring to the example case in Fig. 3, since  $R_e$  coincides with the Thevenin equivalent impedance and the open-circuit voltage is absent, in the  $k$ th step of the simulation the CM solves (6) by an iterative numerical algorithm.

The CM presents the advantage that it avoids any numerical transient. The main drawback is that it needs the evaluation of the value of the Thevenin equivalent impedance at the PV generator terminals in each step of the simulation. This value is available from the linear system solution only if the network is solved by explicit inversion of its admittance matrix. Such an inversion is very heavy in terms of computational burden and therefore it is not used in simulation tools.

#### 4 EXTENDED LINEAR SYSTEM TECHNIQUE

Another approach to overcome numerical problems, namely the ELST, is proposed in the following starting from the methods used to include rotating machines and switching devices in power system simulation [22, 23]. The basic idea is to extend the BLST adding a linear representation of the non-linear equation of the PV generator into the solution of the rest of the power system. The block diagram of the  $k$ th simulation step for the proposed ELST is represented in Fig. 6. The first block is the same as the one in the BLST case: the value  $I_i(k)$  is evaluated by solv-

ing (1) given the value  $V_i(k-1)$  available from the previous step of the simulation. The difference is in the subsequent blocks. While the BLST solves the linear system represented in Fig. 7a, the ELST solves the extended linear system represented in Fig. 7b. The two linear systems differ for the value of the current generator: in the BLST it is equal to  $I_i(k)$  and in the ELST to  $I_g(k)$ . Moreover, the extended linear system presents an additional shunt branch including the voltage generator  $V_d(k)$  and the resistance  $R_d(k)$ . These two components model the linear response of the diode around the operating voltage  $V_i(k-1)$  and are evaluated by

$$R_d(k) = -\left. \frac{\partial I_i(V_i)}{\partial V_i} \right|_{V_i(k-1)}^{-1} = \frac{a}{\beta I_o} e^{-\frac{\beta V_i(k-1)}{a}} \quad (9)$$

$$\begin{aligned} V_d(k) &= V_i(k-1) - R_d(k) I_d(V(k-1)) \\ &= V_i(k-1) - \frac{a}{\beta} \left( 1 - e^{-\frac{\beta V_i(k-1)}{a}} \right). \end{aligned} \quad (10)$$

Consequently, the second block in Fig. 6 evaluates  $V_d(k)$  and  $R_d(k)$  and the third solves the extended linear system to obtain the vector  $\mathbf{V}(k)$  of all nodal voltages.

Referring to the example circuit in Fig. 3, the solution of the extended linear system is

$$V_i(k) = \frac{R_e R_d(k)}{R_e + R_d(k)} \left( I_g + \frac{V_d(k)}{R_d(k)} \right) \quad (11)$$

and, substituting (9) and (10) into (11), it can be easily proved that the  $k$ th step of the simulation results into

$$\begin{aligned} V_i(k) &= R_e \left( I_i(V_i(k-1)) \right. \\ &\quad \left. + \left. \frac{\partial I_i(V_i)}{\partial V_i} \right|_{V_i(k-1)} (V_i(k) - V_i(k-1)) \right) \end{aligned} \quad (12)$$

which is the first order approximation of the Taylor series of (6).

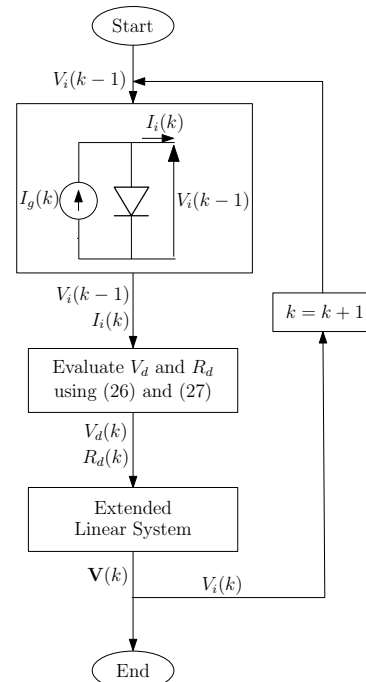
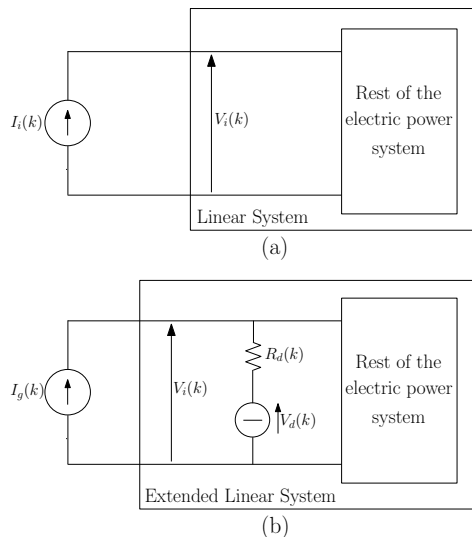


Figure 6: Block diagram of the simulation steps in the proposed ELST.



**Figure 7:** Linear system in BLST (a) and extended linear system in ELST (b), solved at the  $k$ th step of the simulation.

The main advantage of ELST with respect to the CM is the absence of the evaluation of the Thevenin equivalent circuit of the power system. Then, it can be implemented whatever technique is used for the network solution. Existing power system simulation tools can be used, which are very effective in dealing other non-linearities, such as the ones related to switching devices in the PV system.

On the other hand, the ELST introduces numerical transients, due to the approximation of the Taylor series at the first order derivative. Anyway, simulation instability is significantly reduced with respect to the BLST, which uses a zero order derivative approximation.

## 5 NUMERICAL SIMULATION RESULTS

The results of numerical simulation studies are reported to test the performance of ELST with respect to numerical stability. All simulations have been performed using PSCAD/EMTDC with a simulation sampling time equal to  $1 \mu s$ .

A 152 kW PV generator is considered. It is composed of  $N_p = 20$  arrays; each array is composed of  $N_s = 38$  modules by Kyocera of the KC200GT type [24]. The datasheet gives some operational data with reference to the Standard Test Conditions (STC) of irradiance,  $G_r$ , and temperature,  $T_r$ , as reported in Table 1. Referring to the single-diode circuit in Fig. 2, the values of the parameters  $a$ ,  $R_s$ ,  $R_p$ ,  $I_g$  and  $I_o$  are evaluated by using analytical expressions reported in [20] on the basis of the data provided by manufacturers. Table 2 reports the values of the parameters of the single-diode circuit.

The two circuits shown in Fig. 8 are simulated: in case (a) the PV generator supplies a load represented by a variable resistance  $R_e$ ; in case (b) the PV generator is connected to a network equivalent, represented by an impedance including  $R_e$ ,  $L_e$ ,  $C_e$  and a voltage generator  $E_e$ . The values of the electrical parameters of the circuits are reported in Table 3. To test the improvements of numerical stability, the results of simulations performed using both BLST and ELST are compared.

Parameter	Unit	Value
Cell type		multicrystal
$M_s$		54
Open-circuit voltage	(V)	32.9
Short-circuit current	(A)	8.21
Voltage at MPP	(V)	26.3
Current at MPP	(A)	7.61
Voltage/temperature coef.	(V/K)	-0.123
Current/temperature coef.	(mA/K)	3.18

**Table 1:** Data-sheet parameters of the KC200GT module at STC

Parameter	Unit	Value
$a$		1.2
$R_s$	( $\Omega$ )	0.265
$R_p$	( $\Omega$ )	313
$I_g$	(A)	8.22
$I_o$	(A $10^{-9}$ )	21.2

**Table 2:** Parameters of the single-diode circuit for the KC200GT module at STC

Parameter	Unit	Value
$R_e$	( $\Omega$ )	0.01 to 100
$L_e$	(mH)	0.01
$C_e$	( $\mu F$ )	1.0
$E_e$	(V)	850

**Table 3:** Electrical parameters of the circuits in Fig.8

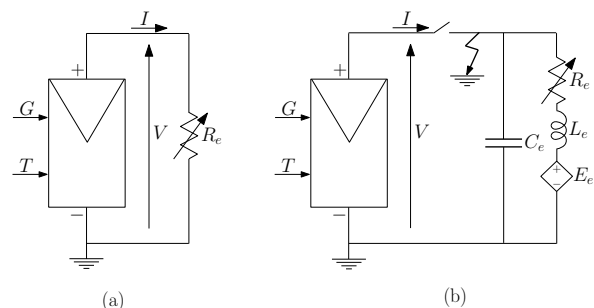


**Figure 8:** Simulated circuits: case (a) and case (b).

In case (a) the numerical stability has been tested with a step variation of the irradiance  $G$  from 100 to  $1000 \text{ W/m}^2$ . The temperature  $T$  has been kept constant and equal to  $25 \text{ }^\circ\text{C}$ . Varying  $R_e$ , it has been observed that the simulation using BLST becomes unstable when  $R_e > 6.6 \Omega$ , that is when  $R_e$  is larger than the value corresponding to the maximum power point at STC. In fact, with such values of  $R_e$ , the PV generator characteristic presents a slope in the  $(V, I)$  plane which is larger in absolute value than the slope of the load characteristic, see (13). On the contrary, the simulation based on ELST has proved to be stable for all the values of  $R_e$ . Assuming  $R_e = 10 \Omega$ , in Fig. 9 the time evolutions of the PV generator voltage  $V$  and current  $I$  are shown around  $t = 0.05 \text{ s}$ , when the step variation of  $G$  occurs. It is apparent that

in few steps of the simulation the numerical transient of ELST is extinguished.

In case (b), the numerical stability has been tested with the same step variation of  $G$  and the same value of  $T$  as the ones of case (a). The simulation based on BLST becomes unstable for values of  $R_e$  higher than  $10 \Omega$ , whereas the simulation based on ELST is always stable. Then, assuming that the PV generator operates at STC, electric transients have been tested, caused by faults and switch opening as represented in Fig. 8b. The simulation based on BLST presents numerical instability when the fault is cleared and when the switch is opened. On the contrary, the simulation based on ELST is stable, although some numerical transients appear. The time evolutions of PV generator voltage and current are shown in Fig. 10: at  $t = 0.05 s$  the fault occurs and it lasts until  $t = 0.1 s$ ; then, at  $t = 0.15 s$  the switch opens and it closes again at  $t = 0.2 s$ . The numerical transients are more significant when the fault is cleared and when the switch is opened. For these two transients, the zoomed time evolutions of voltage and current are shown in Fig 11 and Fig. 12, respectively.

## 6 CONCLUSIONS

The paper tackles the issue of PV system modelling for power system simulation studies. In particular, it investigates the problems of numerical instability caused by the non-linear PV generator model. A new representation of the classical PV generator model, based on the single-diode equivalent circuit, has been proposed. It can be efficiently included into power system simulation tools based on EMTP and EMTDC. The aim is to overcome problems of numerical instability, while keeping high computational efficiency of the simulation. Numerical results have shown the effectiveness of the proposed representation of the PV generator model.

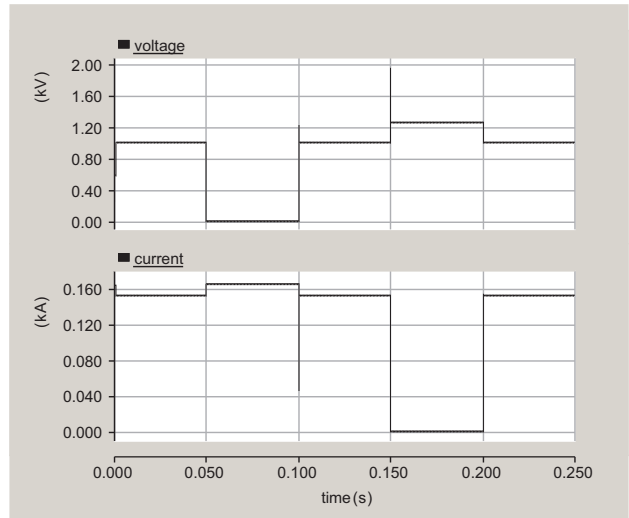


**Figure 10:** Time evolutions of PV generator voltage and current in case (b): all the simulation.

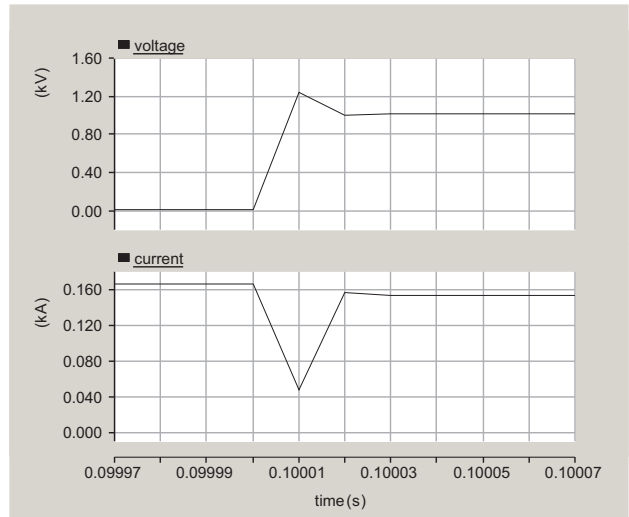


**Figure 11:** Time evolutions of PV generator voltage and current in case (b): fault recovery.

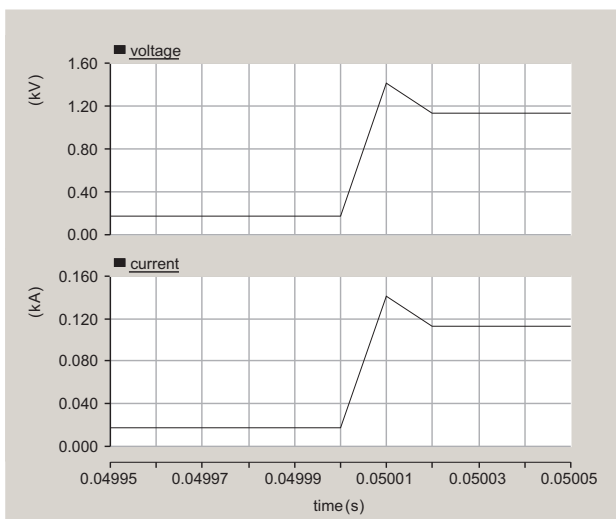


**Figure 9:** Time evolutions of PV generator voltage and current in case (a): step on irradiance.

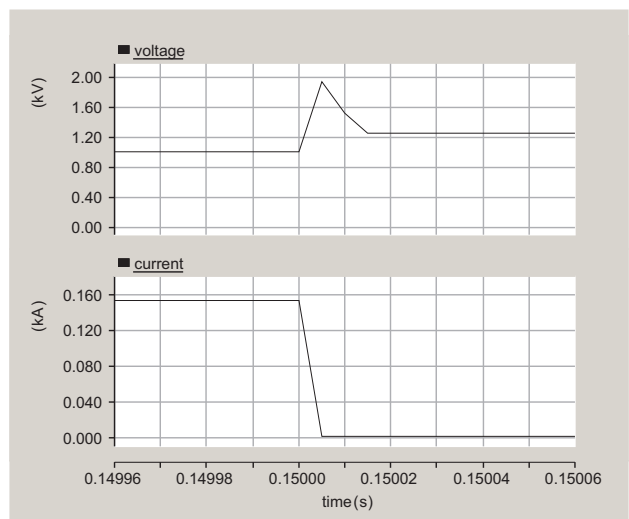


**Figure 12:** Time evolutions of PV generator voltage and current in case (b): switch opening.

## REFERENCES

- [1] J. Duffie and W. Beckman, *Solar Engineering of Thermal Processes*, 2nd ed. New York: John Wiley & Sons, 1991.
- [2] J. Gow and C. Manning, "Development of a photovoltaic array model for use in power-electronics simulation studies," *IEE Proceedings Electric Power Applications*, vol. 146, no. 2, pp. 193–200, 1999.
- [3] K. Nishioka, N. Sakitani, Y. Uraoka, and T. Fuyuki, "Analysis of multicrystalline silicon solar cells by modified 3-diode equivalent circuit model taking leakage current through periphery into consideration," *Solar Energy Materials and Solar Cells*, vol. 91, no. 13, pp. 1222–1227, 2007.
- [4] O. Wasynczuk, "Modeling and dynamic performance of a self-commutated photovoltaic inverter system," *IEEE Transactions On Energy Conversion*, vol. 4, no. 3, pp. 322–328, 1989.
- [5] O. Wasynczuk, "Modeling and dynamic performance of a line-commutated photovoltaic inverter system," *IEEE Transactions On Energy Conversion*, vol. 4, no. 3, pp. 337–343, 1989.
- [6] T. Maris, S. Kourtesib, L. Ekonomou, and G. Fotis, "Modeling of a single-phase photovoltaic inverter," *Solar energy materials and solar cells*, vol. 91, no. 18, pp. 1713–1725, 2007.
- [7] M.E.Ropp and S. Gonzalez, "Development of a matlab simulink model of a single-phase grid connected photovoltaic system," *IEEE Transactions on Energy Conversion*, vol. 24, no. 1, pp. 195–202, 2009.
- [8] Y. Tan, D. Kirschen, and N. Jenkins, "A model of pv generation suitable for stability analysis," *IEEE Transactions On Energy Conversion*, vol. 19, no. 4, pp. 748–755, 2004.
- [9] S. Kim, J. Jeon, C. Cho, E. Kim, and J. Ahn, "Modeling and simulation of a grid-connected pv generation system for electromagnetic transient analysis," *Solar Energy*, vol. 83, no. 5, pp. 664–678, 2008.
- [10] IEEE Task Force on Modeling and Analysis of Electronically-Coupled Distributed Resource Systems, "Modeling guidelines and a benchmark for power system simulation studies of three-phase single-stage photovoltaic systems," to appear in *IEEE Transactions on Power Delivery*.
- [11] M.Park and I. Yu, "A novel real-time simulation technique of photovoltaic generation systems using rtds," *IEEE Transactions on Energy Conversion*, vol. 19, no. 1, pp. 164–169, 2004.
- [12] M. Veerachary, "Psim circuit-oriented simulator model for the nonlinear photovoltaic sources," *IEEE Transactions on Aerospace and Electronic Systems*, vol. 42, no. 2, pp. 735–740, 2006.
- [13] I. Atlas and A. Sharaf, "A photovoltaic array simulation model for matlab-simulink gui environment," in *International Conference on Clean Electrical Power*, 2007, pp. 341–345.
- [14] T. Maguire and A. Gole, "Digital simulation of flexible topology power electronic apparatus in power system," *IEEE Transaction on Power Delivery*, vol. 6, no. 4, pp. 1831–1840, 1991.
- [15] *PSpice User's Guide*, 2nd ed., Cadence Design Systems, Inc., May 2000.
- [16] *EMTDC User's Guide*, Manitoba-HVDC Research Center, April 2005.
- [17] H.W.Dommel, "Non linear and time-varying elements in digital simulation of electromagnetic transients," *IEEE Transactions on Power Apparatus and Systems*, vol. PAS-90, no. 6, pp. 2561–2567, 1971.
- [18] W.F.Tinney, "Compensation methods for network solutions by optimally ordered triangular factorization," *IEEE Transactions on Power Apparatus and Systems*, vol. PAS-91, no. 1, pp. 123–127, 1972.
- [19] *PSCAD User's Guide*, Manitoba-HVDC Research Center, April 2005.
- [20] M. Villava, J. Gazoli, and E. Filho, "Comprehensive approach to modeling and simulation of photovoltaic arrays," *IEEE Transactions on Power Electronics*, vol. 24, no. 5, pp. 1198–1208, 2009.
- [21] D. King, W.E.Boyson, and J. Kratochvil, "Photovoltaic array performance model," Sandia National Laboratories, Tech. Rep. SAND2004-3535, 2004.
- [22] A. Gole, R. Menzies, H. Turanli, and D. Woodford, "Improved interfacing of electrical machine models to electromagnetic transients programs," *IEEE Transactions on Power Apparatus and Systems*, vol. PAS-103, no. 9, pp. 2446–2451, 1984.
- [23] T. Maguire and A. Gole, "Digital simulation of flexible topology power electronic apparatus in power systems," *IEEE Transactions on Power Delivery*, vol. 6, no. 4, pp. 1831–1840, 1991.
- [24] (2010) The KC200GT module datasheet. [Online]. Available: <http://www.kyocera.com/>

## APPENDIX

In BLST, the  $(k + 1)$ th step of the simulation evaluates

$$V_i(k + 1) = R_e I_i(V_i(k)) \quad (13)$$

which, using the first order approximation of the Taylor series of  $I_i(V_i(k))$ , can be written as

$$V_i(k + 1) = R_e I_i(V_i(k - 1)) + R_e \left. \frac{\partial I_i(V_i)}{\partial V_i} \right|_{V_i(k-1)} (V_i(k) - V_i(k - 1)). \quad (14)$$

Substituting (7) in (14) yields

$$V_i(k + 1) - V_i(k) = R_e \left. \frac{\partial I_i(V_i)}{\partial V_i} \right|_{V_i(k-1)} (V_i(k) - V_i(k - 1)). \quad (15)$$

A sufficient condition for convergence poses that

$$|V_i(k + 1) - V_i(k)| < |V_i(k) - V_i(k - 1)| \quad (16)$$

which, standing (15), is satisfied if

$$\frac{1}{R_e} > \left| \left. \frac{\partial I_i(V_i)}{\partial V_i} \right|_{V_i(k-1)} \right|. \quad (17)$$